

# Modeling and Validation of the Effects of Induced Fields in Railguns

Mark Johnson, Paul Cote, and Krystyna Truszkowska  
Benet Laboratories  
Watervliet, NY 12189-4050

*Abstract - The electromagnetic launcher is currently being explored as an alternative to propellant gun systems to satisfy the ordnance requirements of future military systems. Recent improvements in component technologies have increased the plausibility of making the electromagnetic launcher a practical alternative to chemically driven guns. The U.S. Army Armament Research, Development, and Engineering Center's Benet Laboratories has developed an experimental electromagnetic launcher to investigate issues associated with the bore life of rail guns. It serves as an erosion simulator to provide a test bed for validation of new theories on the origins of the dominant erosion mechanisms. A lumped parameter model of the simulator has been developed to provide a means of predicting performance based on the insights provided by experimental findings and a distributed solution of the induced fields. Test results agree very well with predicted behavior and demonstrate that the dominant erosion mechanisms observed in large scale systems can be reproduced on much smaller scale.*

**Keywords:** railgun, erosion, simulation, small-scale launcher, and pulsed power.

## 1. Introduction

Electromagnetic (EM) launchers are currently being investigated as an alternative to conventional solid propellant guns in an effort to address fundamental technical limitations associated with chemical propulsion techniques [1]. EM ordnance systems have the potential to increase projectile velocity, eliminate the propellant storage to enhance platform survivability, provide better control of projectile velocity, and reduce environmental impact. There are a number of EM propulsion technologies including coil guns, rail guns, and linear accelerators. The foundation of all EM guns is based on Lorentz forces that drive the projectiles. Most current research efforts are currently focused on the railgun. The simple railgun is comprised of 2 stationary parallel conductors (rails) and a moving armature. Current flows through the rails and armature producing a

magnetic field between the rails which drives the components apart. Supporting structures keep the rails fixed in place while the armature is free to accelerate. The EM launchers envisioned for use in future military systems require energies that result in damage to both the conducting rails and insulators. The U.S. Army Armament Research, Development, and Engineering Center's (ARDEC's) Benet Laboratories is developing new technologies to enhance the bore life of railguns so that a viable system can be successfully fielded.

## 2. Objective

Cote, et al. [2] conclude that erosion damage to rail surfaces in railguns is primarily due to two main causes: i) edge groove formation from concentrated currents which tend to merge into a central groove, downbore, and ii) relatively uniform thermal damage across the rail faces caused by plasma formation behind the armature. He proposes that induced fields play a dominant role in these erosion effects. The objective of this study is to provide supporting data to validate the conclusion on the origins of edge groove formation.

## 3. Erosion Due to Concentrated Currents

It is commonly observed in rails from firing tests that erosion grooves initially form near the outer edges and gradually converge to a single central groove downbore. Cote, et al. [2] discuss the erosion mechanism in the rail surface in terms of melting enhanced by contact and alloying with hot molten aluminum from the armature. The localization of the erosion into the two grooves at the rail edges and their merging into a single central groove at the downbore locations reflect a similar concentration and merging of the paths of main current through the rail and armature.

## 4. Modeling the Induced Fields

A 3-D model is required to properly describe the essentials of field and current redistributions that arise from induced fields in railguns. A simple model was generated in FEMLAB [3] using an axisymmetric ring of rectangular cross section. FEMLAB is a finite element software package that is based on the solution of partial differential equations for given system configurations, boundary conditions, and material properties. Simplified models are applied for convenience and suffice to provide a description of the essential physics of diffusion effects in bulk armatures and rails. There is no actual motion in the present simple models; it is assumed that the fields in and around the armature are essentially those of this static model because fields propagate at the speed of light. Copper parameters were used for the rail and aluminum parameters for the armatures. One half of the ring was considered to represent a standard C-shaped armature. A 3 ms time duration was used to match typical railgun firing durations. Figure 1 shows the 3-D axisymmetric ring configuration used in the model. The height was set to 4 cm and the radius to 1 cm. A current pulse (loop current) with typical current vs. time profiles for railguns was applied to simulate the effects of time varying currents.

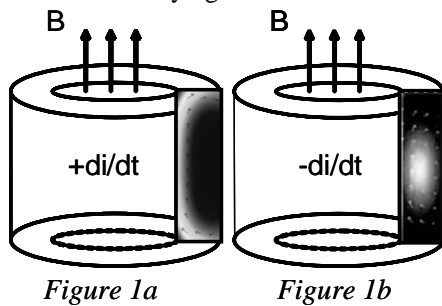


Figure 1. FEMLAB results showing field distributions and ohmic heating due to current concentrations resulting from  $\pm di/dt$ .

The resulting system current initially rises to a peak at approximately 1 ms and then drops off continuously. Figure 1a shows the model result for resistive heating through the armature section at 0.4 milliseconds, during the initial portion of the current pulse, where  $di/dt$  is positive. Also shown is an arrow plot of the magnetic flux density,  $B$ , around the armature. The increasing flux within the ring and the flux that diffuses into the ring induces a back emf that acts primarily near the rear of the armature. The induced current opposes the applied current. The result is a reduction in net current at the rear of the armature, accompanied by a concentration of current and

resistive heating at the top and bottom of the armature. In this case, the current concentrations are most intense at the back corners. Figure 1b shows the resistive heating result at 3.0 ms (well beyond the pulse peak), where  $di/dt$  is negative. As the current is reduced, there is corresponding reduction in magnetic field inside the armature. The resulting decay of the magnetic fields within the armature induces currents within the armature that act to maintain the original currents, in accord with Lenz's law. The induced currents initiate at the top and bottom edges, and migrate towards the center in the negative  $di/dt$  portion of the current plot. The merging of the two induced currents is complete by 3 milliseconds as shown in the resistive heating plot.

## 5. Erosion Simulator Hardware

A small scale launcher has been developed to serve as an erosion simulator to provide a means of validating new perspectives on the dynamic of railguns. Figure 2 shows the pulsed power supply and the corresponding launcher. Power is supplied by switched capacitive energy sources, each coupled with a pulse shaping and current limiting inductance. It is comprised of 4 banks of 20, 3500 $\mu$ F electrolytic capacitors, with each bank coupled to a 10 $\mu$ H inductor. The capacitor banks are sequentially discharged to optimize the current/force profile in an effort to optimize the desired effect. In this study, we stage the banks to investigate the effect of  $di/dt$  on the current distribution. Pickup coils located at the center of each inductor provide a means of measuring the current based on mutual inductance with surrounding coil. The staging sequence is optimized to minimize pickup from the inductors of the other banks. The launcher is based on a design suggested by the Institute of Advanced Technology in Austin, TX. It is 1m (39in) long with a 1in x 0.5in rectangular bore that uses replaceable rail liners and G10 insulators.

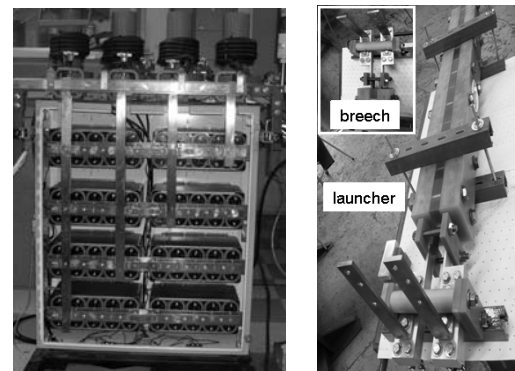


Figure 2. Erosion simulator pulsed power supply and launcher.

## 5.1 Equivalent Circuit Model

Figure 3 shows a block diagram of the equivalent circuit of the launcher. The capacitance ( $C_1$ ), resistance ( $R_1$ ,  $R_2$ ), and inductance ( $L_1$ ) are assumed to be identical for each bank.  $C_1$  represents the 20, 3500 $\mu$ F capacitors in each bank and  $L_1$  is the 10  $\mu$ H bank inductance.  $R_1$  is a combination of the effective series resistance of the capacitors, capacitor fuse resistance, and busbar resistance.  $R_2$  is the resistance of  $L_1$ .  $R_3$  and  $L_2$  are common to all banks.  $R_3$  is the combination of the armature resistance ( $R_{arm}$ ), cable resistance ( $R_{cable}$ ), busbar resistance ( $R_{bus}$ ), breech resistance ( $R_{breech}$ ), armature/rail contact resistance ( $R_{contact}$ ) and rail resistance ( $R_{rails}$ ).  $R_{breech}$  is the resistance of the length of the rail from the breech to starting location of the armature.  $R_{rails}$  is the resistance of the rails from the breech to the back of the armature and increases as the armature travels downbore.  $L_3$  is the total breech inductance ( $L_{breech}$ ), cable inductance ( $L_{cable}$ ), and launcher inductance ( $L_{gun}$ ). Busbar inductance is assumed to be negligible. The values used in the simulation were measured when practical, but were generally estimates based on the geometry and conductivity of the material. Conductance  $G_{eq}$  current source  $I_{eq}$  and source resistance  $r_s$  model a diode that is used in each bank to prevent ringing and damage to the polarized electrolytics. The voltage source,  $idL/dt$ , represents the back EMF due to flux creation that occurs immediately behind the moving armature. The inductance gradient ( $L_x$ ) used to estimate  $L_{gun}$  is assumed to be 0.5  $\mu$ H/m (0.0127  $\mu$ H/in) based on Kerrisk's [4] estimate for the rail geometry.

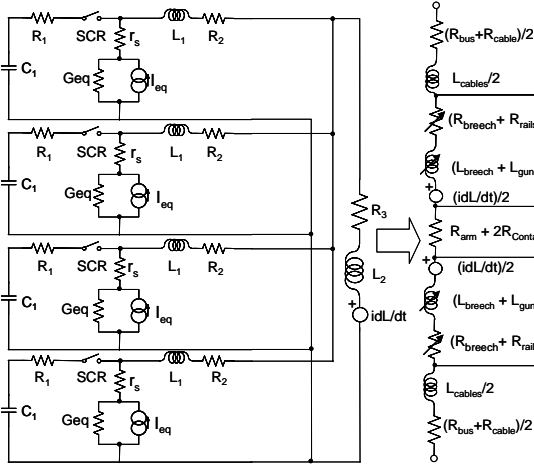


Figure 3. Model of railgun erosion simulator.  
breech voltage =  $v_a - v_b$ , muzzle voltage =  $v_b - v_c$ .

## 5.2 State Space Solution

The model of the erosion simulator is based on transient circuit solutions of sequentially pulsed capacitive energy sources coupled with the Lorentz forces associated with the currents in a sliding contact on parallel conductive rails. The solution of the differential equations involving the state variables associated with the linear storage elements is solved using one step methods while the behavior of nonlinear circuit elements is modeled using an iterative linear companion solution. The linear companion model for the diode is comprised of a parallel combination of conductance,  $G_{eq}$ , and a current source,  $I_{eq}$ . The I-V characteristics of the diode are assumed to be linear at an operating point where  $G_{eq}$  is the slope of the tangent to the I-V curve at the operating point and  $I_{eq}$  is the intercept of the tangent. The correct operating point is determined through convergence of an iterative solution of the nodal equations describing the circuit. The diodes I-V characteristics are given by an ideal Schockley model where:  $I_D = I_S (e^{qV_D/nkT} - 1)$  where  $V_D$  = voltage across the diode and  $I_S$  is the saturation current. The high currents through diode  $D_1$  require that the ohmic resistance,  $r_s$ , of the diode be included in the model. The armature is accelerated by the current in the loop created by the diode and the circuit inductance, as given by the Lorentz force law,  $\frac{1}{2}(dL/dx)I^2$ . A state space solution for the system is given by:

$$\dot{V} = \frac{L_x \sum_{k=1}^n i_L(k)^2}{2m} \quad (1)$$

$$\begin{aligned} \dot{i}_L(k) = & \\ & \frac{i_L(k)(-L_1(R_1 + R_2) - nR_2L_2) + (R_2L_2 - R_3L_1) \sum_{\substack{j=1 \\ j \neq k}}^n i_L(j) +}{L_1(L_1 + L_2(n+1))} \\ & \frac{v_{dp}(k)(L_1 + nL_2) - L_1L_x \sum_{j=1}^n i_L(j) - L_2 \sum_{\substack{j=1 \\ j \neq k}}^n v_{dp}(j)}{L_1(L_1 + L_2(n+1))} \end{aligned} \quad (2)$$

$$\dot{v}_c(k) = \frac{(v_c(k) - v_{dp}(k))}{C} \quad (3)$$

$$v_{dp}(k) = \frac{(v_c(k) - i_L(k)R_1)(G_{eq}(k)r_s + 1) - I_{eq}(k)R_1}{G_{eq}(k)(r_s + R_1) + 1}$$

where  $V$  is the armature velocity,  $i_L(k)$  is the inductor current in bank  $k$ , and  $v_c(k)$  is the capacitor voltage in bank  $k$ ,  $m$  is the projectile mass,  $L_x$  is the inductance gradient, and  $n$  is one less than the number of active banks.

## 6. Results

Figures 4 and 5 show the results of the MATLAB [5] solution for (1)-(3) using parameters representative of Benet's erosion simulation, and experimental measurements. Figure 4 shows  $i_k(k)$  for capacitors charged to an initial voltage of 400 volts and staged to fire at 1ms intervals. 1ms staging was selected based on simulations that show this results in the maximum duration of  $+di/dt$  for our system and therefore the greatest extent of the separation of concentrated currents. Figure 5 shows simulation results for  $di/dt(x)$  and predicts the onset of convergence to begin approximately 3" from the starting location for 1 ms staging.

C-shaped aluminum armatures (6061 alloy) and aluminum rails (6061 alloy) were employed in the tests. Figure 6 is an image that is typical of the distribution of molten armature material on the rails due to the concentrated currents. It shows the onset of convergence begins approximately 1.25in (3cm) from the breech and formation of a central groove at 10in (25cm). Figure 7 shows a laser scanning confocal microscope image of the melt tracks. The image shows that the tracks are deposited armature material, not rail grooves. The energy in our system is insufficient to provide the current necessary to melt the rails, unlike in the larger EM launchers. However, the effect of the induced fields on the distribution of current is the same. The test results associated with the 22.4 kJoule, 1ms staging test were repeatable, and therefore, the effect of varying  $di/dt$  on the distribution of concentrated currents was tested. Simulation results predict that a 20 kJoule, 0.5ms staging configuration result in the same peak current as a 22.4kJoule, 1ms staging configuration. Figure 5 shows predicted onset of convergence for this configuration begins at 1.75 in (4.4cm), from the starting location. This occurs approximately 41% earlier than when 1ms staging is used. Figure 8 shows the test results for the 0.5ms

staging. The onset of convergence of the melt tracks begins at approximately 0.75in, 40% earlier than with 1ms staging.

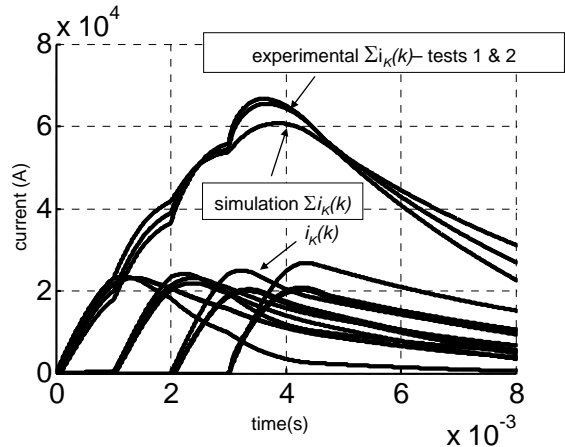


Figure 4. Predicted and measured current history for a 22.4 kJoule, 1ms staging configuration.

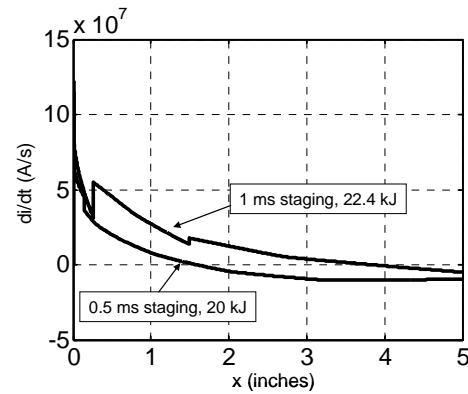


Figure 5. Estimate of  $di/dt$  for 22.4 kJoule, 1ms staging and 20 kJoule, 0.5ms staging configurations.

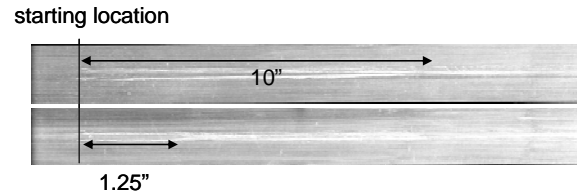


Figure 6. Melt tracks on 2 rails showing the effects of the distribution of concentrated currents for a 22.4 Joule, 1ms staging configuration.

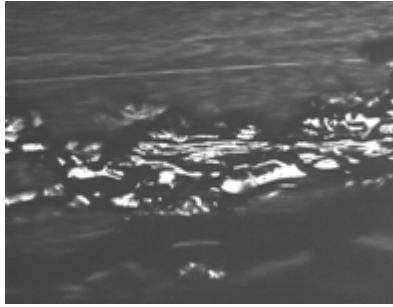


Figure 7. Laser Scanning Confocal Microscope image typical of the distribution of molten armature material along the tracks.

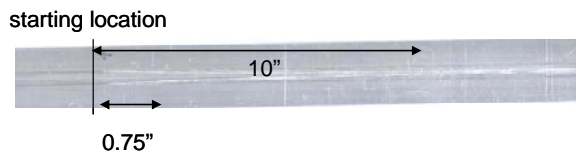


Figure 8. Melt tracks showing the effects of the distribution of concentrated currents for a 20 kJoule, 0.5ms staging configuration.

## 7. Summary and Conclusions

A primary mechanism of damage to the rails surfaces in railguns is a result of concentrated currents. Ohmic heating initially generates grooves along the rail edges, which tend to merge into a single central groove, downbore. A multiphysics model captures the essential physics of diffusion effects to explain this process in terms of current redistributions that arise from induced fields. At start up, as the current is rapidly increasing, the back emf at the rear of the armature tends to drive the current away, towards the top and bottom.

The current is symmetrically distributed at the top and bottom. As the current decreases with time, the resulting transient emfs tend to drive the current to the center of the armature. The excellent agreement between our experimental and simulation results provide additional support for this new theory. These results also show that the dominant wear mechanisms present in larger scale launchers can be reproduced on a much smaller scale. While the onset of convergence occurs in only a few cm on our small scale system, it is evident in the 3-4m launchers at approximately 1m, which is consistent with the onset of negative  $di/dt$  for these systems.

Although more testing is required, our results have provided valuable insight into the dynamics of the system which are useful in identifying the dominant wear mechanisms of the rails. Additional testing is currently underway, and new techniques are being developed to mitigate rail damage. The lumped models, distributed multiphysics models and the erosion simulator promise to be useful resources in our efforts to enhance the bore life of electromagnetic launchers.

## 8. References

- [1] L. Stiefel, "Gun Propulsion Technology", American Institute of Aeronautics and Astronautics, 1988
- [2] P.J. Cote, M.A. Johnson, S. B. Smith, K. Truszkowska, and P. Vottis, "On the Role of Induced Fields in Railguns", internal report ARAEW-TR-05017 (2005).
- [3] FEMLAB is a registered trademark of COMSOL AB.
- [4] J.F. Kerrisk, "Current Distribution and Inductance Calculation for Railgun Conductors", Los Alamos National Laboratory report LA-9092-MS (October 1980)
- [5] MATLAB is a registered trademark of the Mathworks, Inc.